The Effects of Ion Implantation Through Very Thin Silicon Oxide Films

I. J. R. Baumvol
Instituto de Física, Universidade Federal do Rio Grande do Sul
91501-970, Porto Alegre, RS, Brasil

F. C. Stedile
Instituto de Química, Universidade Federal do Rio Grande do Sul
91501-970, Porto Alegre, RS, Brasil

S. Rigo, J.-J. Ganem and I. Trimaille
Groupe de Physique des Solides, Université Paris 7 et 6
75251 - Paris - France

Received January 3, 1994; revised April 20, 1994

The ion implantation of heavy dopant species through very thin silicon oxide gate insulators degrades the insulating properties of the oxide inducing an enhanced leakage current in MOS siructures as well as a decrease of the dielectric breakdown voltage. In the present work we study quantitatively the possible physico-chemical causes of these degradation phenomena and of their recovery by thermal annealing using ^{18}O isotopic tracing techniques. Films of $Si^{18}O_2$ with thicknesses ranging from 4 to 10 nm thermally grown on (100) silicon wafers were irnplanted with As and Sb to fluences between 10^{14} and 10^{16} cm^{-2}. Using nuclear reaction aialyses, secondary ions mass spectrometry, nuclear resonance profiling and channeling of α-particles with detection at grazing angles we measured the amount of oxygen lost from the silicon dioxide films due to sputtering at the oxide-vacuum interface, the amounts of oxygen recoil-implanted into silicon from the oxide film and into the silicon oxide from the residual gas in the implantation chamber, and the change in the stoichiometry of the silicon dioxide films due to through-oxide implantation. The results of the present work together with the results existing in the literature on the electrical characterization of the same systems are used to discuss the possible physico- chemical causes of the observed dielectric loss, and some preliminary results on the recovery of the dielectric characteristics of the oxide films by thermal annealing in oxygen atmospheres after implantation are also discussed.

I. Introduction

It is usual in silicon semiconductor devices produced in very large scale integration (VLSI) technology to perform the ion implantation of the active silicon surface regions across the gate dielectric, which consists of a silicon dioxide film thermally grown from the silicon substrate before ion implantation. The silicon semiconductor devices produced in VLSI technology require silicon oxide layers to be used as gate dielectrics with thickness of 10 nm and below. Such ion implantation through the very thin gate oxide is known to cause a most undesirable degradat on of the dielectric characteristics of the silicon oxide, as it has been largely reported in the literature for the case of metal-oxide-semiconductor (MOS) structures following arsenic source/drain ion implantation at typical fluences from 1×10^{15} to 1×10^{16} $As.cm^{-2}$ [1-4] . The phenomenon is unique to MOS structures where the gate edges are over regions of thin oxide as is typical for self-aligned source/drain implants depicted in Fig. I.

The implantation-induced dielectric degradation manifests itself by a lowering of the breakdown voltage and an increase of the prebreakdown leakage current in MOS devices (Fig.2). The magnitude of the degradation is greatest following implants of heavier dopants (As,Sb), while lighter dopants (B,P) produce a much smaller effect. Furthermore, significant changes of the

above mentioned dielectric characteristics were only observed for gate oxides thiner than 12 nm. At and above that thickness the effects of through oxide ion implantation were seen to be very small[1].

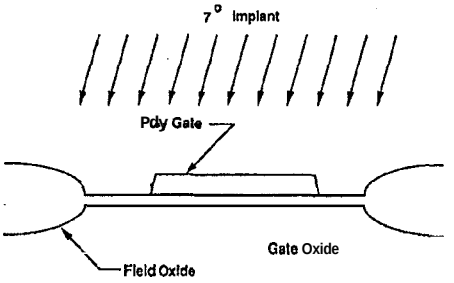

Figure 1: A polysilicon gate MOS structure of the kind addressed in this study with the gate edge overlaying the very thin gate oxide dielectric film. The implants are normaly performed at 7° tilt in order to avoid implantation in a clianneling direction. (From Ref.2).

In the search for the possible mechanisms to explain the implantation-induced degradation previous authors have considered the defects produced in the oxide by the crossing implanted ions, the implantation-induced gate charging, stress effects, recoiled atoms and ion mixing. Of those, mainly oxide damage and displacement of oxygen and silicon atoms associated with collisions can be considered as significant causes. Atomic displacement, in particular, can alter the stoichiometry of the SiO_2 film and it has been well demonstrated the enhanced conductivity of nonstoichiometric silicon oxide films. For example a 7% silicon-rich oxide film formed by chemical vapour deposition (CVD) was found to conduct a current of 400 $\mu A.cm^{-2}$ at 4 $MV.cm^{-1}$, whereas a stoichiometric, thermally grown film conducts current of only picoamperes at this field[5]. Atomic displacement can also produce mixing at the SiO_2-Si interface, altering the chemistry of the interface and consequently its electrical properties. The theory of ballistic mixing (recoil implantation) estimates for 50 keV As implants through an oxide film 10 nm thick one oxygen recoil into the underlying silicon per incident implant ion[6]. Thus a typical As junction implantation of 3×10^{15} cm^{-2} would displace about 10% of the oxygen atoms from a gate oxide film, thereby allowing for a disruption of the oxide stoichiometry and a significant contamination of the near to the interface silicon layers. Furthermore, the film thickness is reduced by an amount which can be by itself responsible for most of the observed dielectric loss.

For the present and future stages of VLSI technology it becomes decisive to reestablish the dielectric quality of silicon oxide after implantation, and so the adequate post-implantation treatment is also searched. To achieve this aim a clear understanding of the mechanisms of dielectric degradation is necessary, especially because the scale rules set a trend for a further decrease of the gate oxide thickness.

Although reasonably well identified from a qualitative point of view, the possible mechanisms for implantation-induced dielectric loss have not been so far well characterized from a quantitative point of view. This lack of a good quantitative picture of the various phenomena occurring in the above described physical situation can be attributed to the rather poor sensitivity of the available methods to measure concentrations, stoichiometric ratios and depth profiles of oxygen in the near to the surface regions and to the shadowing of some of these phenomena by reoxidation in air of the implanted MOS structures.

In the present work we study quantitatively the atomic transport of oxygen in thermally grown SiO_2 films on silicon substrates due to through-oxide ion implantation with As and Sb. The film thicknesses were in the range between 4 and 10 nm and the quantities to be measured are the oxygen lost by sputtering at the SiO_2-vacuum interface, the oxygen recoil-implanted from the SiO_2 films into silicon substrates, the oxygen recoil-implanted from the residual gas in the implantation chamber into the SiO_2 film, the change in thickness of the SiO_2 films and the change in stoichiometry of these films. In order to make the present measurements we grew thermally the SiO_2 films in O_2 gas isotopically enriched to 97% with ^{18}O, so eliminating possible shadowing effects due to reoxidation in air. Other important experimental improvements used here were i) the measurement of the concentration versus depth profiles of ^{18}O by combining secondary ions mass spectrometry (SIMS) which has very high sensitivity unless for the very near surface region, with the profiling by means of the $^{18}O(p,\alpha)^{15}N$ nuclear resonance at 151 KeV which

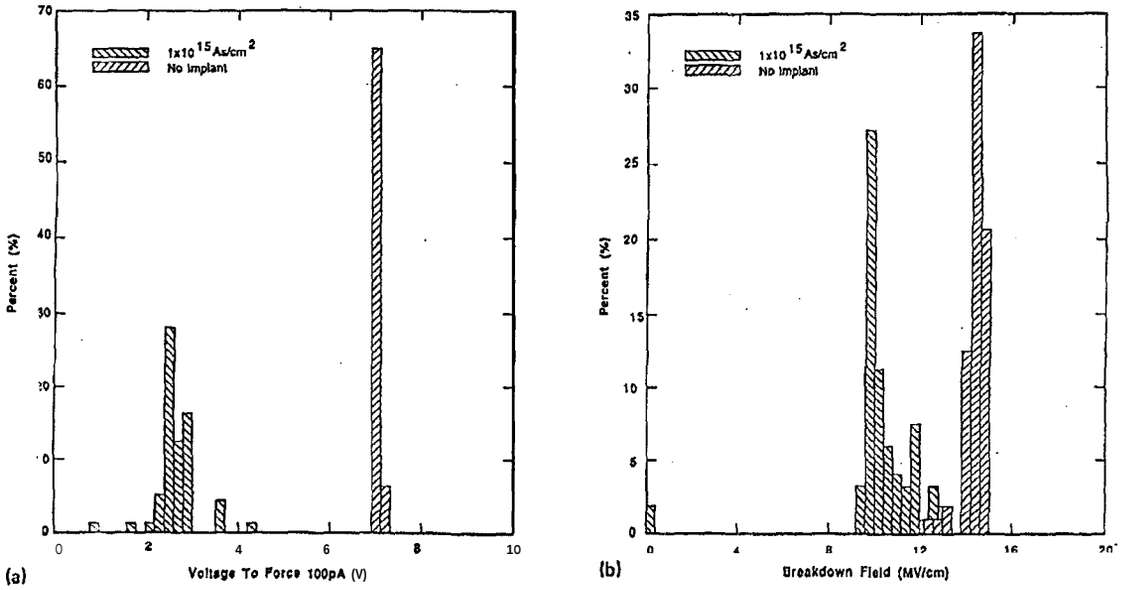

Figure 2: Histograms obtained from 200-μm square capacitors with 7.5 nm silicon oxide dielectric films of: (a) the voltage needed to force 100 pA through the gate oxide dielectric in unimplanted and through-oxide implanted samples: (b) dielectric breakdown for unimplanted and through-oxide implanted samples. (From Ref. 7).

presents very good sensitivity near to the surface; and ii) the deterinination of the oxygen/silicon stoichiometric ratios of the oxides by means of the combination of channeling of α-particles along the crystallographic axis of the underlying silicon substrate with the detection of the backscattered a-particles at grazing angles.

On the basis of our results we present a discussion of the relative magnitude of each one of the possible effects of ion implantation through very thin gate oxides that contribute to its dielectric degradation, and we report on preliminary results of thermal reoxidation of the implanted structures aimed to recover the dielectric characteristics of the film.

II. Experimental procedures

II.1 Samples preparation

The silicon oxide films used in the present work were prepared by rapid thermal oxidation (RTO) of (100) silicon wafers, using a furnace at the Groupe de Physique des Solides, Université Paris 7, that could be pumped down to pressures in the range of 10^{-7} Pa and after pressurized with oxygen gas that could be recovered after the RT3 procedure. The O_2 gas used for the oxidations wâs enriched to 97% with the 180 isotope. All the oxidations were performed at a temperature of 1050°C, pressures of O_2 in the range between 8000 and 14000 Pa, for times between 60 and 160 s. The resulting films had thicknesses between 4 and 10 nm, with an uniformity in the central region of the wafer better than 5%.

Immediately before RTO the silicon wafers were submitted to a chemical etching cleaning procedure in a solution of HF-ethanol followed by rinse in ethanol. This procedure removes completely the native oxide and slows down significantly the regrowth of this oxide.

II.2 Ion implantation, thermal annealings and removal of oxides

The ion implantations were performed in the silicon oxide on silicon samples in different ion implanters, namely the 200 KeV ion implanter of Université Paris XI at Orsay, the HVEE-400 KeV ion implanter at Porto Alegre, and the 250 KeV ion implanter at Bagneux. The implantation energies were chosen to be 100 KeV for As and 140 KeV for Sb, which according to TRIM calculations would give a projected range of 60 nm (much larger than the oxide thicknesses) for both species. The pressure in the implantation chambers were always below 10^{-4} Pa and implantation current

densities were typically in the range of 1 $\mu A.cm^{-2}$.

Thermal annealings of the implanted samples were always performed before oxide removal. A classical furnace was used, which could also be kept in ultra-high vacuum ($P < 10^{-5} Pa$) during the annealing. Typical temperatures for thermal annealing of the samples were in the range between 700 and 800°C and times between 10 and 60 min. The criterion for choosing the thermal annealing parameters was given by the analysis of the annealed samples with channeling of 1.5 MeV a-particles, requiring complete epitaxial regrowth of the silicon layer amorphised by ion implantation and also a near to 100% substitutionallity of the implanted species.

In many cases the remaining oxide layer after ion implantation and thermal annealing was removed by chemical etching in a diluted HF solution in water. The etching times necessary to completely remove the oxide were established in each case, ranging around 30 s.

11.3 Analytical methods

The total amounts of ^{16}O and ^{18}O were measured by nuclear reaction analysis (NRA) using the 2.5 MeV Van de Graaf accelerator of the Groupe de Physique des Solides, Université Paris 7, using energies corresponding to plateaus in the cross sections of the used nuclear reactions. For the determination of the total amounts of ^{16}O, the $^{16}O(d,p)^{17}O$ reaction at deuteron energies of 810 KeV was used. The detection angle of the protons was 90^0 and a 13 μm mylar foil was placed in front of the detector to stop the backscattered deuterons. A $Si^{16}O_2$ standard having 5.7×10^{17} $^{16}O.cm^{-2}$ was used and this method has a sensitivity of 10^{14} $^{16}O.cm^{-2}$. The total amounts of ^{18}O were measured using the $^{18}O(p,\alpha)^{15}N$ nuclear reaction at proton energies of 730 KeV. The detection angle of the a-particles was 165° and a 13 mm thick mylar foil was placed in front of the detector. A $Ta_2^{18}O_5$ standard having 2.55×10^{17} $^{18}O.cm^{-2}$ was used and this method has a sensitivity to ^{18}O of 10^{12} cm^{-2} [7].

The depth profiles of ^{18}O were measured by secondary ions mass spectrometry (SIMS) at the laboratories of IBM-France, where only the profiles after removal of the oxide were measured. Nuclear resonance profiling was alternatively used by means of the 151 KeV resonance of the $^{18}O(p,\alpha)^{15}N$ nuclear reaction ($\Gamma = 100$ eV), using the proton beam of the HVEE-400 KeV ion implanter at Porto Alegre. A highly tilted sample geometry was used for the measurements (70°) in order to increase the length of the trajectory of the incident protons in the oxide films. The α-particles were detected at 90° with respect to the direction of incidence of tlie proton beam. A 3 μm thick mylar foil was placed in front of the detector to stop the backscattered protons[7].

The stoichiometry of the silicon oxide films was measured by a very convenient combination of channeling of 1.5 MeV a-particles along the < 100 > axis of the underlying silicon substrate with the detection of the scattered a-particles at a very grazing angle (95° with tlie direction of incidence of the beam). This method has been largely discussed by Feldman and co-workers[8,9] and it is perhaps unique in determining precisely the stoichiometry of very thin films of silicon oxide on silicon substrates.

III. Experimental results

III.1 Total amounts of oxygen

Table I gives the total amounts of ^{18}O and ^{16}O as measured by NRA in silicon oxide films of various different thickness before and after through oxide implantation with As (100 KeV, 3 x 10^{15} cm^{-2}) and Sb (140 KeV, 1 x 10^{15} cm^{-2}), as well as in the implanted samples after the removal of the remaining oxide layers by means of chemical etching.

One can see that the total amounts of ^{16}O for the different initial oxide thicknesses remains more or less constant before and after implantation and are reduced to a smaller (also more or less constant) value after oxide removal. They represent the ^{16}O previously existing in the silicon wafers plus that incorporated by thermal oxidation and reoxidation in air as well as that due to recoil implantation from the residual gas in the implantation chamber. The constancy on the total amounts of ^{16}O reveals the very little influence of all these factors in the composition of the oxide films.

The amount of oxygen removed from the samples by sputtering at tlie oxide-vacuum interface due to the

implanted ions is essentially given by the difference between the total amount of ^{18}O in the initial oxide filnz and that remaining in tlie film after implantation. Table II shows that sputtering can be responsible for a thinning of t ıe initial oxide films by amounts that vary from 15 to 30%, depending on the initial oxide thickness and on the implantation parameters. In general the heavier implanted species (Sb) is more efficient in removing oxygen atoms by sputtering than the ligliter one (As).

The amoiint of oxygen recoil implanted into the silicon substrate is essentially represented by the total amounts of ^{13}O remaining in tlie samples after tlie removal of the oxide layer. The amounts of ^{18}O recoil-implanted into silicon do not depend significantly on the initial oxide thickness, whereas Sb implantation is again much more efficient than As in recoil-implanting oxygen.

Table II shows the effect of the implantation doses of As and Sb bcth in oxide thinning by sputtering and in the recoil-implantation of oxygen into silicon. A $Si^{18}O_2$ film of initial thickness of 7.4 nm was used. The implantation doses varied from 7×10^{14} to 1×10^{16} cm^{-2}. It is seen in Table II that the thinning of the oxide films and the amoiints of oxygen recoil-implanted into silicon have a dramatic increase at the higher implantation doses.

111.2 Oxide stoichiometry

The changes in the stoichiometry of the implanted oxide films with respect to the stoichiometry of the unimplanted f lms were measured by means of channeling of 1.5 MeV a-particles along the < 100 > crystallographic axis of the underlying silicon substrate, in the grazing angle detection geometry of tlie backscattered a-particles. The experimental procedure consisted in first submittir g the implanted samples to furnace annealing in ultra- high vacuum for epitaxial regrowth of the silicon surface layer that was amorpliised by the ion implantation procedure. The annealing temperatures were rather moderate (around 700°C) and the annealing times were chosen such as to lead in each case to tlie complete epitaxial regrowth of the amorphised layer, whiclz was verified again by channeling of a-particles iii the < 100 > axis, with detection of the backscattered particles at 165° with respect to the direction of incidence of the beam. After reaching a complete epitaxial regrowth, the channeling measurements with grazing angle detection were accomplished and the stoichiometry of tlie films was determined according to tlie analysis described in Refs. 8 and 9.

An example is given in Fig. 3 were we show the < 100 > oriented backscattering spectra of 1.5 MeV incident a-particles detected at 95° with respect to the direction of incidence of the beam. In Fig. 3a it is shown the spectrum obtained from a silicon oxide film thermally grown by RTP in a 97% ^{18}O enriched O_2 gas (P = 8400 Pa, T = 1050°C, t = 60 s). The areas of the signals coiresponding to Si, ^{18}O and ^{16}O were calculated and the analytical procedure described in Refs. 8 and 9 leads to a $(^{18}O + ^{16}O)$ / Si ratio of 2.02 ± 0.2, confirming the perfectly stoichiometric composition of the thermally grown silicon dioxide films. In Fig. 3b it is shown the spectrum obtained from the same film after: i) As implantation to a dose of 3×10^{15} cm^{-2}; ii) annealing at 700°C for 60 min in ultra-high vacuum; and iii) confirmation of the complete epitaxial regrowth of tlie amorphised layer by channeling and a 100% substitutionallity of tlie implanted As ions. The calculation of tlie areas of the ^{18}O, ^{16}O and Si signals in the experimental spectrum and the same analysis made for the unimplanted sample gives in this case a $(^{18}O + ^{16}O)$ / Si ratio of 1.86 ± 0.3, revealing that after implantation the silicon dioxide film became significantly oxygen deficient

Tlie same kind of analysis was made in several different tlirough-oxide implanted samples and the results gave always non-stoichiometric films deficient in oxygen. The oxygen/silicon ratios in the through-implanted films varied from 1.6 to 1.9, depending on the initial oxide thickness and the implantation dose and species. Not a clear correlation between implantation parameters and filrns composition was obtained in this case.

Table I - The total amounts of ^{18}O and ^{16}O (in units of 10^{15} atoms.cm^{-2}) in the as thermally grown silicon dioxide films on silicon samples, and the total amounts of these isotopes in the corresponding samples after ion implantation and after ion implantation and oxide removal by chemical etching. The total thickness of the oxide films was calculated using the equivalent thickness of silicon dioxide: 1 x 10^{15}O.cm^{-2}=0.225 nm. The total amounts of ^{18}O were determined with a precision better than 1% and those of ^{18}O with a precision better than 5%.

Initial Oxide Film			After Ion Implantation				After Ion Implantation and Oxide Removal			
			3 x 10^{15}As.cm^{-2}		1 x 10^{15}Sb.cm^{-2}		3 x 10^{15}As.cm^{-2}		1 x 10^{15}Sb.cm^{-2}	
^{18}O	^{16}O	Total Thickness	^{18}O	^{16}O	^{18}O	^{16}O	^{18}O	^{16}O	^{18}O	^{16}O
10^{15} cm^{-2}		(nm)	10^{15} cm^{-2}				10^{15} cm^{-2}			
20.1	1.9	4.9	14.0	2.2	16.5	2.7	2.1	1.1	1.9	1.3
23.3	2.4	5.7	16.3	2.8	19.6	2.9	2.6	1.3	2.2	1.3
31.2	2.0	7.4	22.1	2.6	26.8	2.6	2.8	1.2	3.1	1.4
39.4	2.2	9.3	26.2	2.7	28.3	2.3	2.3	1.7	2.9	1.1

Table II - The total amounts of ^{18}O and ^{16}O (in units of 10^{15} atoms.cm^{-2}) in 7.4 nm thick silicon dioxide films (31.2 x 10^{15} ^{18}O.cm^{-2}) as thermally grown silicon oxide and the total amounts of these isotopes on these samples after through oxide implantation with As and Sb at various fluences before and after removal of the remaining oxide layer after implantation.

Implantation Dose As,Sb (10^{15}cm^{-2})		^{18}O After Ion Implantation ^{18}O(10^{15}cm^{-2})		^{18}O After Ion Implantation and Oxide Removal ^{18}O(10^{15}cm^{-2}	
As	Sb	As	Sb	As	Sb
1.0	0.7	26.0	28.1	0.9	0.9
3.0	1.0	22.1	26.8	2.8	2.6
6.0	3.0	19.0	22.0	3.4	3.3
10.0	6.0	17.1	18.8	13.5	13.3

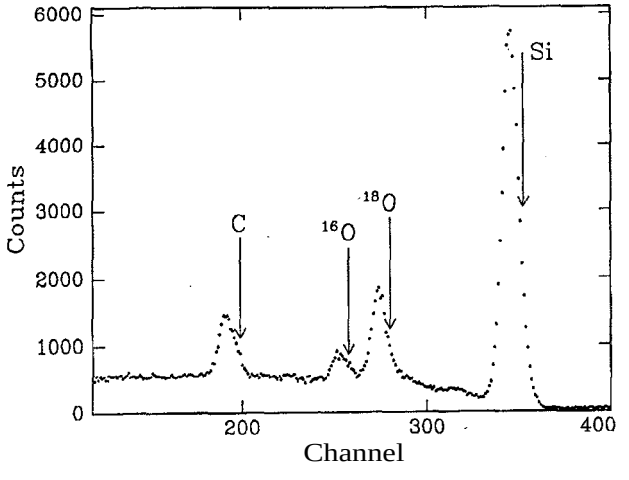

Figure 3: Channeling and grazing angle detection: the spectrum of α-particles scattered from a 4.9 nm thick silicon oxide film grown on a (100) silicon wafer, with the 1.5 MeV incident α-particle beam oriented along the < 100 > axis and the scattered particles detected at 95° with the direction of incidence of the beam. The arrows indicate the surface position of the different elements appearing in the spectrum. The carbon peak is due to the contamination of the sample in air and during the implantation process; it remains in the outermost surface of the sample.

111.3 Concentration versus depth profiles

The concentration versus depth profiles of the ^{18}O atoms recoil-implanted from the silicon oxide films into the silicon substrate were measured before and after removal of the oxide as well as before and after thermal annealing of the implanted samples. SIMS and nuclear resonance profiling were used.

In Fig. 4 we show the excitation curves for the $^{18}O(p,\alpha)^{15}N$ nuclear reaction measured for the 7.4 nm $SiO_2$2 film as grown and after through-implantation with As and Sb to different doses. These curves can he converted into concentration versus depth profiles by the methods described in Ref. 10, but for the purposes of the present work it is satisfactory only to introduce an approximate depth scale calculated on the basis of the energy loss of protons in silicon dioxide. The excitation curve for the unimplanted oxide film presents a clear plateaus which corresponds to the homogeneous concentration region of the silicon dioxide film. The progressive thinning of the oxide at increasing implan-

tation doses is also apparent from the inspection of Fig. 4, as well as the introduction of small amounts of ^{18}O into silicon due to recoil implantation.

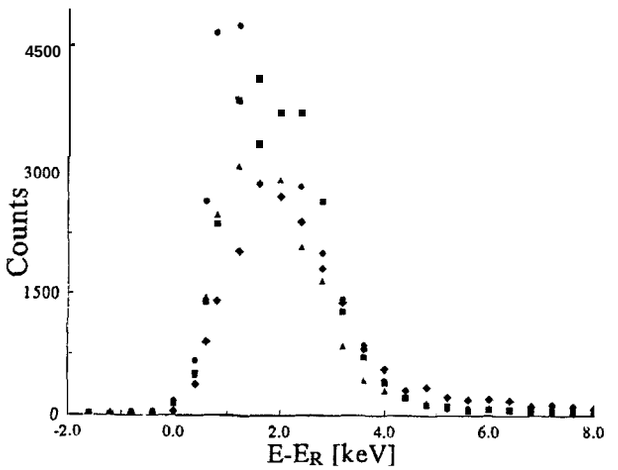

Figure 4: The excitation curves of the **151** keV resonance (E_R= **151.2** keV, Γ_R = **100** eV) in the $^{18}O(p,\alpha)^{15}N$ nuclear reaction measured for the as-grown 7.4 nm thick silicon oxide film on a silicon substrate (•) and for the same film implanted with 100 keV As ions at fluences of 1 x 10^{15} cm^{-2} (■), 6×10^{15} cm^{-2} (A) and 1×10^{16} cm^{-2} (♦). The samples were tilted by 60° with respect to the direction of incidence of the beam. The E − E_R scale can be converted into a depth scale: E' − E_R = 1 keV corresponds to 2.6 nm.

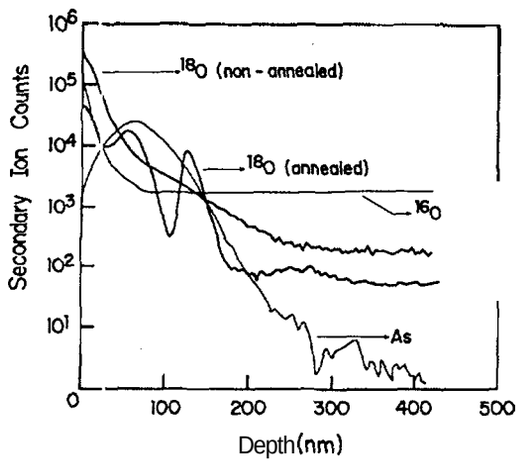

Figure 5: Deptli profiles as measured by secondary ions mass spectrometry (SIMS) after oxide removal, for a through-oxide implanted silicon oxide on silicon film (4.9 nm thick). The profiles of ^{18}O were measured for the sarnple immediately after implantation with As ions (**100** keV, 3 × 10^{15} cm^{-2}) as well as after ion implantation followed by thermal annealing in ultra-high vacuum at 700°C during **60 min.** The ^{16}O and As profiles were measured only for the implanted and annealed sample.

The concentration profile of the recoil implanted ^{18}O into silicon measured by SIMS for the case of As implantation is given in Fig. 5, where we show the ^{18}O profiles after oxide removal for the implanted and non-annealed and for the implanted and annealed samples. Also shown are the ^{16}O and ^{75}As profiles which are not significantly altered by annealing. One notice in Fig. 5 the redistribution of ^{18}O in the silicon substrate after thermal annealing: the surface concentration of ^{18}O decreases almost one order of magnitude; the profile is exponential-like before annealing, while it shows two pronounced peaks after annealing, one at the depth of the maximum concentration of the implanted arsenic and another at the depth corresponding to the previous amorphous-crystalline interface. It is however well known that the SIMS technique has extremely poor sensitivity in the first few nanometers below the surface because of the instabilities in the sputtering process. For this reason the depth profiles of recoil-implanted atoms into the silicon substrate were measured after oxide removal by the alternative technique of the $^{18}O(p,\alpha)^{15}N$ nuclear resonance profiling. The advantage is that, by using a highly tilted sample geometry (70°) we can reach very high sensitivity and depth resolution in the first 10 nm below the surface, so complementing the informations obtained by SIMS. Fig. 6 shows the excitation curves for the case of through-oxide implantation with As ions in non-annealed and annealed samples after oxide removal.

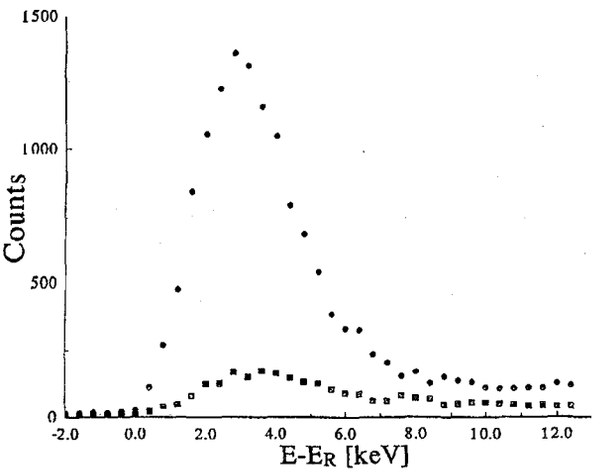

Figure **6:** The excitation curves ofthe **151** keV resonance in the $^{18}O(p,\alpha)^{15}N$ nuclear reaction measured after oxide removal, for the through-oxide implanted samples with As ions (**100** keV, 1 × 10^{16} cm^{-2}). After implantation only **(e)**, and after implantation followed by thermal annealing in ultra-high vacuum at 700°C during 60 min (■). The samples were tilted by 70° with respect to the direction.

IV. Discussion and conclusions

The results here obtained reveal that the through-oxide implantation of heavy dopant species of silicon like As and Sb cause severe physico-chemical changes in the oxide films which can explain most of the observed dielectric degradation of the films. Apart of the defects produced in the oxide by the implanted ions, which have not been considered here, we can discuss from a quantitative point of view these other modifications of the oxide films.

First of all we have determined that As and Sb implantation through the oxide films remove oxygen atoms by sputtering at the oxide-vacuum interface by amounts that vary from 10% of the total number of oxygen atoms initially existing in the films, at the lower implantation doses, to 50% at the higher implantation doses. This thinning effect did not manifest itself as an important cause of dielectric loss in MOS structures when oxides of 20 nm or thicker were used., However, as the initial oxide thickness was reduced to 10 nm or less, the ion implantation to the higher doses performed here can reduce the effective oxide thickness in the device to a point that turns the electric field in the dielectric (for the typical bias voltages used in the corresponding MOS device gates) higher than that allowed by the dielectric strength of the oxide, even if it would be stoichiometric.

Another important effect of through-oxide implantation is the recoil implantation of oxygen atoms from the film into the underlying silicon substrate. We showed that the recoil- implanted oxygen atoms are confined to a very shallow region beneath the oxide-silicon interface (a few nanometers deep), with one peak of concentration at that interface, and so even for the rather small amounts of oxygen recoil-implanted into silicon at the lower implantation doses, their concentration near to the interface reaches several atomic percent which creates a non-stoichiometric transition zone between the dielectric film and the semiconductor substrate which conducts far more electric current than the sharp dielectric- semiconductor interface existing previously to implantation. This effect becomes catastrophic for the higher implantation doses (above 6×10^{15} cm^{-2} for As implants, for instance) where more than 30% of the oxygen atoms in the film are recoil-implanted into silicon, leading to very high concentrations of oxygen in silicon near to the oxide-semiconductor interface. We also showed that the oxygen atoms recoil-implanted into silicon are redistributed by thermal annealing, occupying specific regions of the doped silicon layer and so altering also the semiconductor properties of the silicon active zone.

Furthermore we have demonstrated that the through-oxide ion implantation of As and Sb changes the stoichiometry of the initially perfectly stoichiometric silicon dioxide films. The oxide films are oxygen-defective after implantation, having stoichiometries between $SiO_{1.6}$ and $SiO_{1.9}$ after thermal annealing in vacuum. This is well known to be a cause of enhanced electrical conductivity in the oxide, an effect which has been reported in the literature for the specific case of silicon oxide.

In conclusion we have measured individual and quantitatively several different possible causes of the dielectric degradation of silicon dioxide due to through-oxide implantation, such that one can examine the efficacy of each one of these possible causes by comparison with the measured dielectric characteristics of the through-implanted oxide films.

We have also performed preliminary thermal annealings of the through-implanted oxide films in an oxygen atmosphere (using pure $^{16}O_2$ gas in order to be able to separate the effect of reoxidation with ^{16}O during thermal annealing from the $Si^{18}O_2$ films remaining after implantation) trying to recover the original thicknesses and stoichiometries of the oxide films. We have, however, kept the annealing temperatures and time intervals which can activate the dopants without major redistribution of their concentration versus depth profiles. This is a very strict requirement of VLSI technology which cannot be overcome. The result was that the amounts of ^{16}O incorporated in the films were not enough to restore the oxide thickness and stoichiometry, consistently with the literature where several reports show the difficulties in recovering the original dielectric properties of the silicon dioxide films after through oxide ion implantation. We will continue these experiments by trying to perform rapid thermal annealings in oxygen atmospheres at much higher temperatures than

the ones used so far.

Acknowledgments

This work was supported in part by CNPq, CAPES and FAPERGS-Brasil and by GDR86 of CNRS-France.

References

1. S. Sugiura and S. Shinozaki, J. Electrochem. Soc. 134, 681 (1987).
2. M. G. Stinson and C. M. Osburn, J. Appl. Phys. 67, 4190 (1990).
3. H. L. Peek and J. F. Verwey, in Insulating *Films* on Semiconductors, edited by J.J. Simone and J. Buxo (Elsevier Publishers, Amsterdam, 1986) pg. 199.
4. D. Flcwers, J. Electrochem. Soc. **134**, 698 (1987).
5. D. W. Dong, E. A. Irene and D. R. Young, J. Electrochem. Soc. 125, 819 (1978).
6. R. A. Moline and A. G. Cullis, Appl. Phys. Lett. 26, 551 (1975).
7. F. C. Stedile, I. J. R. Baumvol, S. Rigo, J.-J. Ganem, I. Trimmaile and G. Battistig, *Ion* Beam Analysis of Very Thin Silicon Nitride and *Oxini*-tride Films, Appl. Surf. Sci., to be published.
8. L. C. Feldman, J. Silverman, J. S. Williams, T. E. Jackman and I. Stensgaard, Phys. Rev. Lett. 41, 1396 (1978).
9. N. W. Cheung, L. C. Feldman, P. J. Silverman and I. Stensgaard, Appl. Phys. Eett. 35, 859 (1979).
10. G. Battistig, G. Amsel, I. Trimaille, J.-J. Ganem, S. Rigo, F. C. Stedile and I. J. R. Baumvol, High Resolution Low Energy Resonance Depth *Profiling of* ^{18}O in Near Surface Isotopic Tracing Studies, Nucl. Instrum. Meth., to be published.